PAPER Nr.: 86

Theoretical and Experimental Studies on System Identification of Helicopter Dynamics

Anzhong TAN and Tadahiro KAWADA
Aviation Division, Kawada Industries, Inc., Tokyo, Japan

Akira AZUMA
Azuma Institute of Aeronautical Science, Tokyo, Japan

and

Shigeru SAITO and Yoshinori OKUNO
Flight Research Division, National Aerospace Laboratory, Tokyo, Japan

TWENTIETH EUROPEAN ROTORCRAFT FORUM
OCTOBER 4 - 7, 1994 AMSTERDAM

Printed by the Technical Highschool Haarlem

Theoretical and Experimental Studies on System Identification of Helicopter Dynamics

Anzhong TAN and Tadahiro KAWADA
Aviation Division, Kawada Industries, Inc., Tokyo, Japan

Akira AZUMA
Azuma Institute of Aeronautical Science, Tokyo, Japan

and

Shigeru SAITO and Yoshinori OKUNO
Flight Research Division, National Aerospace Laboratory, Tokyo, Japan

Abstract

Extensive theoretical and experimental studies were performed on the system identification of helicopter dynamics. The linearized equations of motion of helicopters were nondimensionalized by using fundamental parameters related to helicopter dynamics. The derivatives were numerically obtained from a helicoper flight simulation code utilizing perturbation method. Some derivatives are nonlinear which may introduce errors to the linearized system analysis. It is shown that the accuracy of system identifications may be improved in case the squared terms of velocities and angular velocities are added in the linearized equations. Flight tests were performed with Robinson R22 and Eurocopter AS 332 L-1 Super Puma. The necessary flight data were collected from various sensors placed in the helicopters and stored into a portable data acquisition system. The derivatives then were experimentally determined by solving the equations for the measured control inputs and outputs of the motions of the helicopters. The numerical results and the experimental results were compared and discussed in this paper.

Nomenclature

a	= lift slope
B	= tip loss factor
g	= gravitational acceleration
L, M, N	= moments arround x, y, z axes, respectively
p, q, r	= angular velocities arround x, y, z axes, respectively
R	= main rotor radius
u, v, w	= velocities in x, y, z directions, respectively
x, y, z	= aircraft fixed coordinates
X, Y, Z	= forces in x, y, z directions, respectively
Φ, Θ, Ψ	= Euler angles from earth fixed coordinates to aircraft fixed coordinates
ρ	= air density
τ	= nondimensional time scale
ψ	= blade azimuth angle
θ_t	= twist angle of main rotor blade
θ_{0M}	= main rotor collective pitch angle
θ_C	= lateral cyclic pitch angle
θ_S	= longitudinal cyclic pitch angle
θ_{0T}	= tail rotor pitch angle
Ω	= rotational speed of main rotor

subscripts

H	= corresponding to horizontal stabilizer
M	= corresponding to main rotor
T	= corresponding to tail rotor
V	= corresponding to vertical stabilizer
0	= at trimmed flight

superscripts

$\dot{()}$	= time derivative
$\bar{()}$	= nondimensional variable
$()'$	= nondimensional time derivative for nondimen-sional variable

1. Introduction

The flight dynamics of a helicopter is very complicated for its fully three-dimensional moving freedom. Generally, a helicopter is dynamically unstable and is controllable only by trained pilots. It is desirable to have stability augmentation system (SAS) or automatic stability equipment (ASE) installed to improve the stability of the aircraft. However, the highly nonlinear equations of motion are very difficult to analyze directly. For stability analysis, it is desirable to describe the dynamics of the helicopter in linearized state variable form. The number of variables or degrees of freedom used to model the helicopter dynamics is 14 in the case of UH-60 identification [1] which includes inflow/engine/governor, flapping and lead-lag freedoms along with the basic fuselage model. Even with this extensive system, the simulated outputs do not perfectly coincide with the measured flight data. There appear to be many sources that introduce errors into the measured flight data. Also different methods adapted to identify the stability derivatives can lead to different results. The most widely accepted validation for the identified model is to compare the simulated response with the dissimilar flight data. However, the identified model may seems valid for a set of flight data but not for another. More investigations are required to understand the unique flight characteristics of the helicopters.

The so-called state or stability derivatives obtained from the flight data may lack accuracy because the helicopter is dynamically unstable and requires control corrections at all times. The control induced flight deviations are dominant in flight data. It is not possible to give the helicopter a sudden known attitude or velocity or angular velocity change without moving the controls and with other axes states fixed. Stability derivatives estimated via analysis may be more reliable to be used in stability analysis and stability augumentation system designs. However, careful attention must be paid to the applicable limitations of analysis. Especially, off-axis response is often reported not to agree with flight data[2].

In this paper, the analytical estimation of the stability derivatives are studied and a set of nondimensional parameters for the linearized equations of motions is proposed. It is numerically shown that some nonlinear terms exist to make the motion of helicopter nonsymmetrical and the accuracy of system identification may be improved when these terms are included.

2. Analytical derivatives estimation

Basic equations of motion

The coordinates used to describe the motion of a helicopter are shown in Figure 1. The origin of the aircraft axes is placed on the center of gravity of the aircraft excluding the rotor blades. The motion of the rotors are analyzed separately, and the forces and moments from the rotors are considered as external forces and moments acting at the rotor hubs.

The helicopter is assumed to be a rigid body

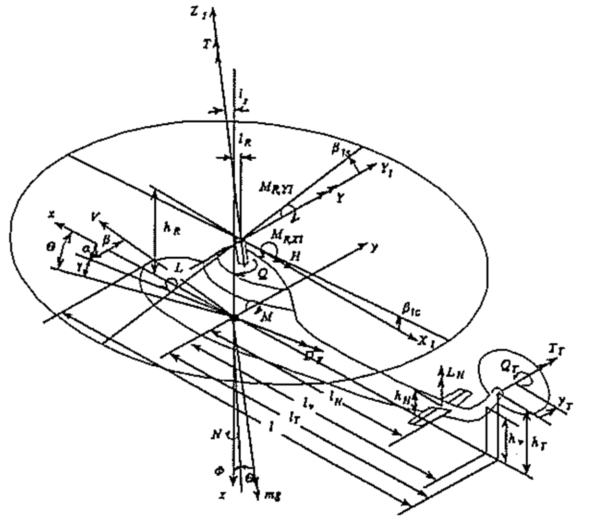

Figure 1 Helicopter coordinates

which gives the basic equations of motion as

$$
\begin{aligned}
&X - mg\sin\Theta = m(\dot{u} + qw - rv)\\
&Y + mg\cos\Theta\sin\Phi = m(\dot{v} + ru - pw)\\
&Z + mg\cos\Theta\cos\Phi = m(\dot{w} + pv - qu)\\
&L = I_{xx}\dot{p} - I_{xz}\dot{r} + (I_{zz} - I_{yy})qr - I_{xz}pq \qquad (1)\\
&M = I_{yy}\dot{q} + (I_{xx} - I_{zz})rp + I_{xz}(p^2 - r^2)\\
&N = I_{zz}\dot{r} - I_{xz}\dot{p} + (I_{yy} - I_{xx})pq + I_{xz}qr
\end{aligned}
$$

The forces and moments *X, Y, Z, L, M, N* are the sum of the aerodynamic forces and moments from the rotors, the stabilizers and the aircraft fuselage. A complete set of analytical expressions are derived for the aerodynamic forces and moments of the rotors based on the classic blade element theory. The inversed flow region and root cut-out corrections are included in the expressions. However, the induced flow by the rotor is a function of the forces and moments and the blade flapping angles are also coupled. Therefore, calculations are inherently iterative.

<u>Trim analysis</u>

The forces and moments acting on the helicopter are calculated as the summation of all the forces and moments of the aerodynamical components. Trim analysis is used to compute the required control positions and attitude of the aircraft which make the total forces and moments to be equal to zero for the subscribed flight conditions.

A trim analysis and flight simulation program named 'AnaHeliAero' has been developed by authors which uses fully analytically integrated rotor formulas as the basis of computation. Flight condition parameters are velocities and angular velocities which can be defined on the aircraft body-fixed axes or earth-fixed axes. The parameters used to describe the helicopter include the rotational direction of both the main rotor and tail rotor. The rotor swashplate tilt plane angle shift from the body axis is also considered. The rotor type can be defined as seesaw rotor, rigid rotor, or the Robinson type rotor for which delta three hinge setting for flapping is different from that of teetering.

For the vertical or sideway flight of the helicopter, the induced flow of main or tail rotor based on normal momentum theory is no longer valid. Following rotor vortex ring state model is included in this computer program.

$$
\frac{V_D}{v_0} = \left(\frac{v}{v_0}\right)^{C_1}\sin^2\alpha_R \pm \sin\alpha_R\cdot\sqrt{\left(\frac{V_D}{v}\right)^2 - \left(\frac{v}{v_0}\right)^2\left(C_2\sin^2\alpha_R + \cos^2\alpha_R\right)} \qquad (2)
$$

where $v_0 = \sqrt{C_T/2}$ and V_D is rate of decent for the rotor. α_R is the attack angle of the rotor plane and v here is for induced flow velocity.

Eq.(2) is the extension to the Glauert's momentum theory[3]. In computations, $C_1 = 0.3$, $C_2 = 0.25\cdot(1+\sqrt{2})^{-4}$ are used to fit to Azuma et al's experimental results[4].

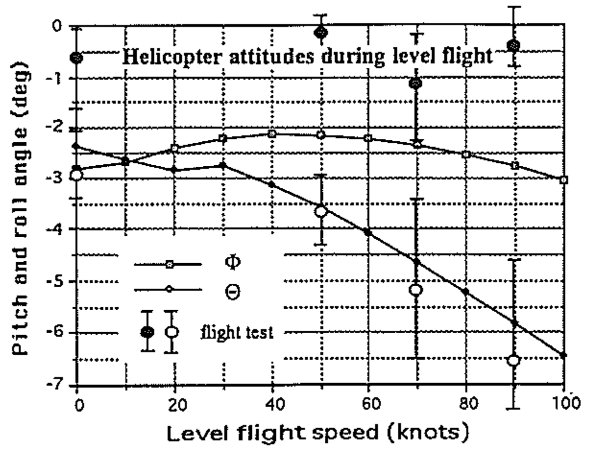

(a) Helicopter attitudes

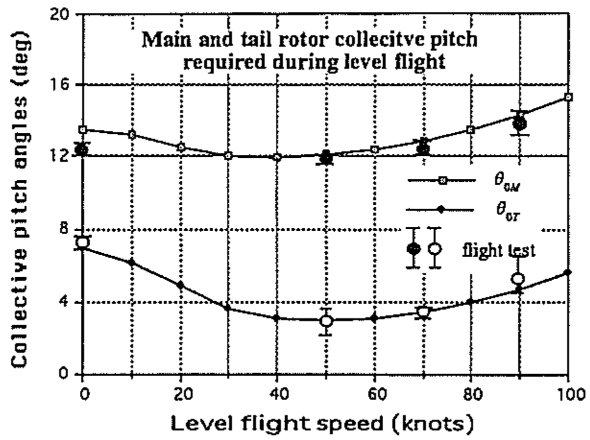

(b) Main and tail rotor collective pitches

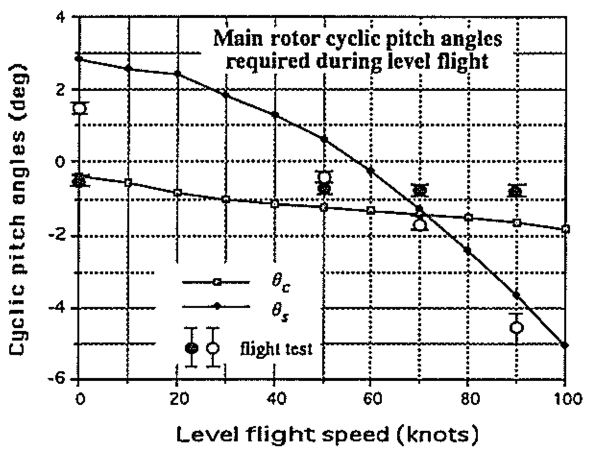

(c) Cyclic pitch angles

Figure 2 Trim analysis results for Robinson R22 helicopter

The trim analysis is performed by defining the six forces and moments components as the dependent function of the totally six control and attitude independent variables (three main rotor control inputs, one tail rotor control and two aircraft attitudes). Newton's method is applied in this case to compute the required independent variables corrections to make the forces and moments to be zero. The derivatives required in Newton's method are estimated by giving small changes to the controls and attitudes separately and calculating the changes of forces and moments. The same idea is used to estimate the stability derivatives required for the stability analysis. Although this approach requires some extra computational time, results showed that the trim analysis iteration converges well and is very robust for the strong cross-coupling problem.

The trim analysis results for Robinson R22 are shown in Figure 2. Flight test results are also plotted in the same graph for comparison. The typical flight parameters for Robinson R22 are shown in Table 1.

Table 1 Typical parameters for Robinson R22 at flight test

Item	Notation	Quantity	Unit
Mass of Helicopter	m	554.0	kg
Inertia about x axis	Ixx	99.1	kg*m^2
Inertia about y axis	Iyy	361.5	kg*m^2
Inertia about z axis	Izz	322.4	kg*m^2
C.G. x arm*	Xcg	0.065	m
C.G. y arm*	Ycg	-0.034	m
C.G. z arm*	Zcg	1.58	m
Main rotor rotation rate	Ω	508.6	RPM

* Center of gravity position relative to main rotor hub

The discrepancies found in Figure 2, especially for roll angles is quite large. The possible reason may be that in the test, the helicopter was not flying completely level and straight forward. Even a small amount of side slip can change the attitude of this small helicopter quite significantly. However, the required controls computed agree with the flight test results quite well.

This program is also used for the trim analysis of AS 332 L-1. Although only detailed hovering flight test was carried out by the time of this report, the test result meet with the computational results quite well.

<u>Nondimensional linearized expressions</u>

Following small perturbation linearization procedure, the motion of a helicopter around trimmed flight can be expressed as:

$$\dot{\mathbf{u}}(t) = \dot{\mathbf{u}}_0 + \mathbf{C}_g\Theta(t) + \mathbf{A}\mathbf{u}(t) + \mathbf{B}\theta(t) + \mathbf{C}_{u_0}\mathbf{p}(t) \qquad (3)$$

where

$$\mathbf{u}(t) = [u, w, q, v, p, r]^{\mathrm{T}}$$

$$\mathbf{C}_g = \begin{bmatrix} -g & 0 & 0 & 0 & 0 & 0 \\ 0 & 0 & 0 & g & 0 & 0 \end{bmatrix}^{\mathrm{T}}$$

$$\Theta(t) = [\Theta, \Phi]^{\mathrm{T}}$$

$$\mathbf{A} = \begin{bmatrix} X_u & X_w & X_q & X_v & X_p & X_r \\ Z_u & Z_w & Z_q & Z_v & Z_p & Z_r \\ M_u & M_w & M_q & M_v & M_p & M_r \\ Y_u & Y_w & Y_q & Y_v & Y_p & Y_r \\ L_u & L_w & L_q & L_v & L_p & L_r \\ N_u & N_w & N_q & N_v & N_p & N_r \end{bmatrix}$$

$$\mathbf{B} = \begin{bmatrix} X_{\theta_{0M}} & X_{\theta_S} & X_{\theta_C} & X_{\theta_{0T}} & X_{\Omega} \\ Z_{\theta_{0M}} & Z_{\theta_S} & Z_{\theta_C} & Z_{\theta_{0T}} & Z_{\Omega} \\ M_{\theta_{0M}} & M_{\theta_S} & M_{\theta_C} & M_{\theta_{0T}} & M_{\Omega} \\ Y_{\theta_{0M}} & Y_{\theta_S} & Y_{\theta_C} & Y_{\theta_{0T}} & Y_{\Omega} \\ L_{\theta_{0M}} & L_{\theta_S} & L_{\theta_C} & L_{\theta_{0T}} & L_{\Omega} \\ N_{\theta_{0M}} & N_{\theta_S} & N_{\theta_C} & N_{\theta_{0T}} & N_{\Omega} \end{bmatrix}$$

$$\theta(t) = [\theta_{0M}, \theta_S, \theta_C, \theta_{0T}, \Omega]^{\mathrm{T}}$$

$$\mathbf{C}_{u_0} = \begin{bmatrix} -w_0 & 0 & v_0 \\ u_0 & -v_0 & 0 \\ 0 & 0 & 0 \\ 0 & w_0 & -u_0 \\ 0 & 0 & 0 \\ 0 & 0 & 0 \end{bmatrix}$$

$$\mathbf{p}(t) = [q, p, r]^{\mathrm{T}}$$

Note that the derivatives in this equation are dimensional parameters. For analysis, it is desirable to have these equations nondimensionalized to make the coefficients in the matrices have same order of magnitude. Similar to the fixed-wing aircraft analysis, the basic nondimensional scales are selected as $R\Omega$ for velocity, $\tau = \frac{R\Omega}{g}\cdot\frac{\overline{W}}{\sigma} = \frac{m}{\rho S_b(R\Omega)}$ for time, where σ is solidity of the rotor as $\sigma = \frac{bc}{\pi R}$. Then the scale for distance becomes $R\Omega\tau$.

For the fixed-wing, the representative time is defined as $\tau = \frac{m}{\rho SV}$. For helicopter, we can see the flight speed is corresponding to $R\Omega$ and wing area S to blade area S_b.

The nondimensional scales for R22 and AS 332 L-1 are listed in Table 2.

Table 2 Nondimensional scales

Parameter	Robinson R22	AS 332 L-1	Unit
m	554	7,000	kg
b	2	4	—
R	3.83	7.79	m
Ω	508.6	265	rpm
RΩ	204.0	216.2	m/s
τ	1.61	1.41	s
τ^2	2.59	1.99	s^2
1/RΩ	0.0049	0.0046	s/m
τ/RΩ	0.0079	0.0065	s^2/m
$R\Omega\tau^2$	528.4	430.2	m s

From Table 2, we can see that the nondimensional scales for R22 and AS 332 L-1 are nearly the same dispite their weights are different by a factor as large as 12. Conventional helicopters usually have similar blade tip speed and the blade loading also fall into the same order. This makes the nondimensional scales do not differ so significantly as the fixed-wing aircraft. However, the flight dynamical characteristics for different types of helicopter can be compared more easily in nondimensional forms. With the above nondimensional scales, Eq.(3) can be written as

$$\bar{\mathbf{u}}'(\bar{t}) = \bar{\mathbf{u}}'_0 + \bar{\mathbf{C}}_g\bar{\Theta}(\bar{t}) + \bar{\mathbf{A}}\bar{\mathbf{u}}(\bar{t}) + \bar{\mathbf{B}}\bar{\theta}(\bar{t}) + \bar{\mathbf{C}}_{\bar{u}_0}\bar{\mathbf{p}}(\bar{t}) \qquad (4)$$

The derivatives are nondimensionalized as

$$\bar{X}_{\bar{\Theta}} = -g\frac{\tau}{R\Omega}, \ \bar{Y}_{\bar{\Phi}} = g\frac{\tau}{R\Omega};$$

$$\bar{X}_{\bar{u}} = X_u\tau, \ \bar{X}_{\bar{q}} = X_q\frac{1}{R\Omega}, \ \bar{X}_{\bar{\theta}_s} = X_{\theta_s}\frac{\tau}{R\Omega};$$

and

$$\bar{L}_{\bar{v}} = L_v R\Omega\tau^2, \ \bar{L}_{\bar{p}} = L_p\tau, \ \bar{L}_{\bar{\theta}_c} = L_{\theta_c}\tau^2.$$

Numerical derivatives estimation

The derivatives can be estimated numerically by changing the flight condition or control inputs in the flight simulation program 'AnaHeliAero'. The changes of forces and moments caused by the small parameter deviation from the trim condition are the numerical estimations for the desired derivatives. Because the computer simulation program 'AnaHeliAero' is completely based on nonlinear relations, the derivatives estimated depend on the amount of the parameter deviation. Figure 3 shows the numerically estimated derivatives changes with the quantity of parameter deviations near hover for R22.

It can be seen from Figure 3 that some stability derivatives changes drastically with the deviation of parameter. Z_u and Z_v showed to have negative values with Δu and Δv. It means that horizontal translation velocities always gives the rotor more lift. Analytical formulation for rotor thrust validate this result for it has squared terms for advance ratio. The state changes that give the rotor vertical velocities also cause its derivatives to be highly nonlinear because the induced flow by the rotor is inherently nonlinear and also the empirical equations for vortex-ring state cause the motion nonsymmetrical. In this hovering case, control derivatives are nearly constant, which means linearization of these terms are reasonable. However more than half of the state derivatives are highly nonlinear.

The derivatives for R22 at 70 knots level flight are shown in Figure 4. Nonlinear derivatives are much less than those at hovering flight. Only N_w and N_q have clearly dependence on parameter deviation. If the perturbation range is limited, it can be seen from Figure 4 that it is suitable to use linearized equation of motion for this case.

Such numerical estimation results for the derivatives imply that special care must be given to the system identification of the heli-

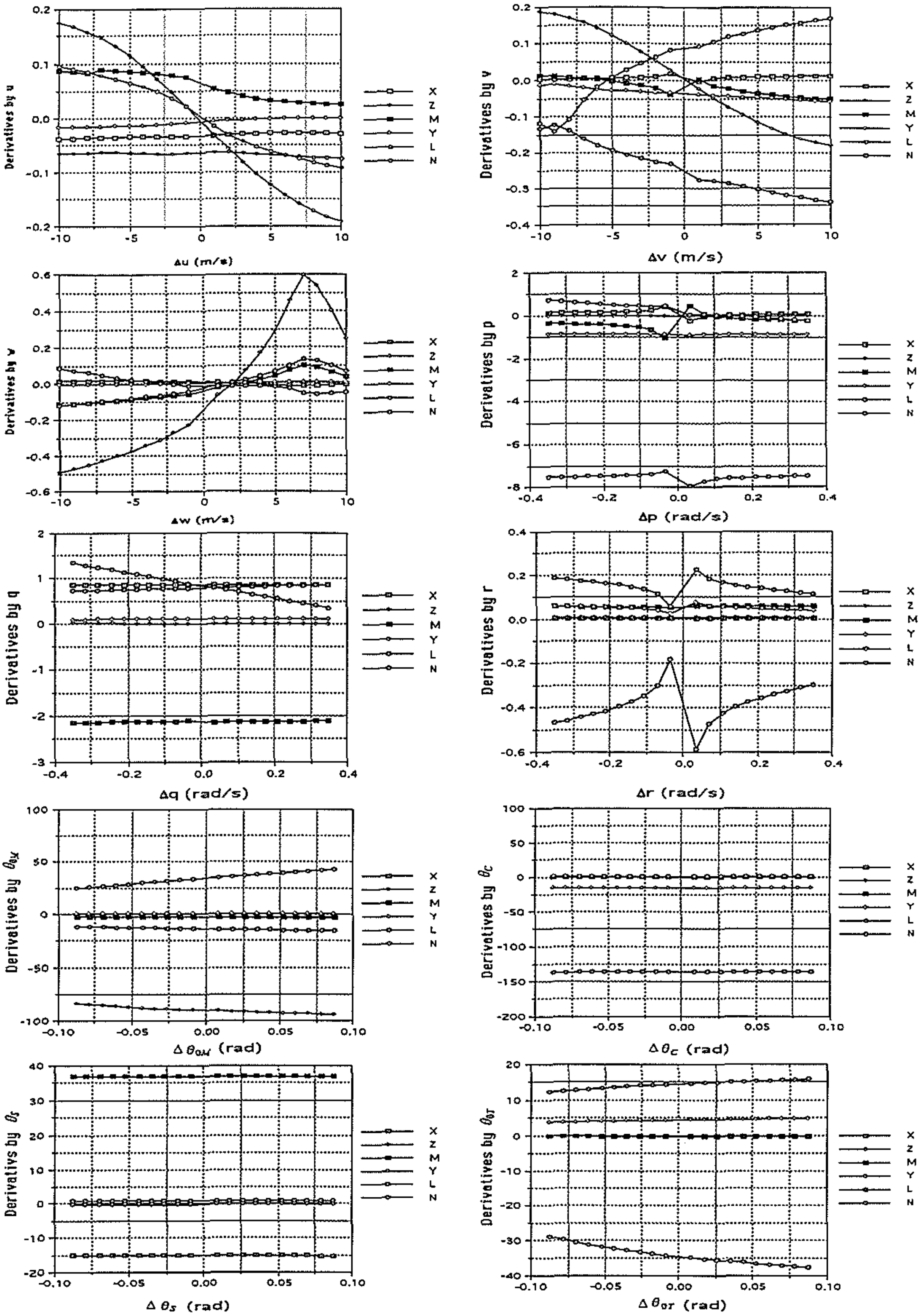

Figure 3 Numerically estimated derivatives in hover for Robinson R22

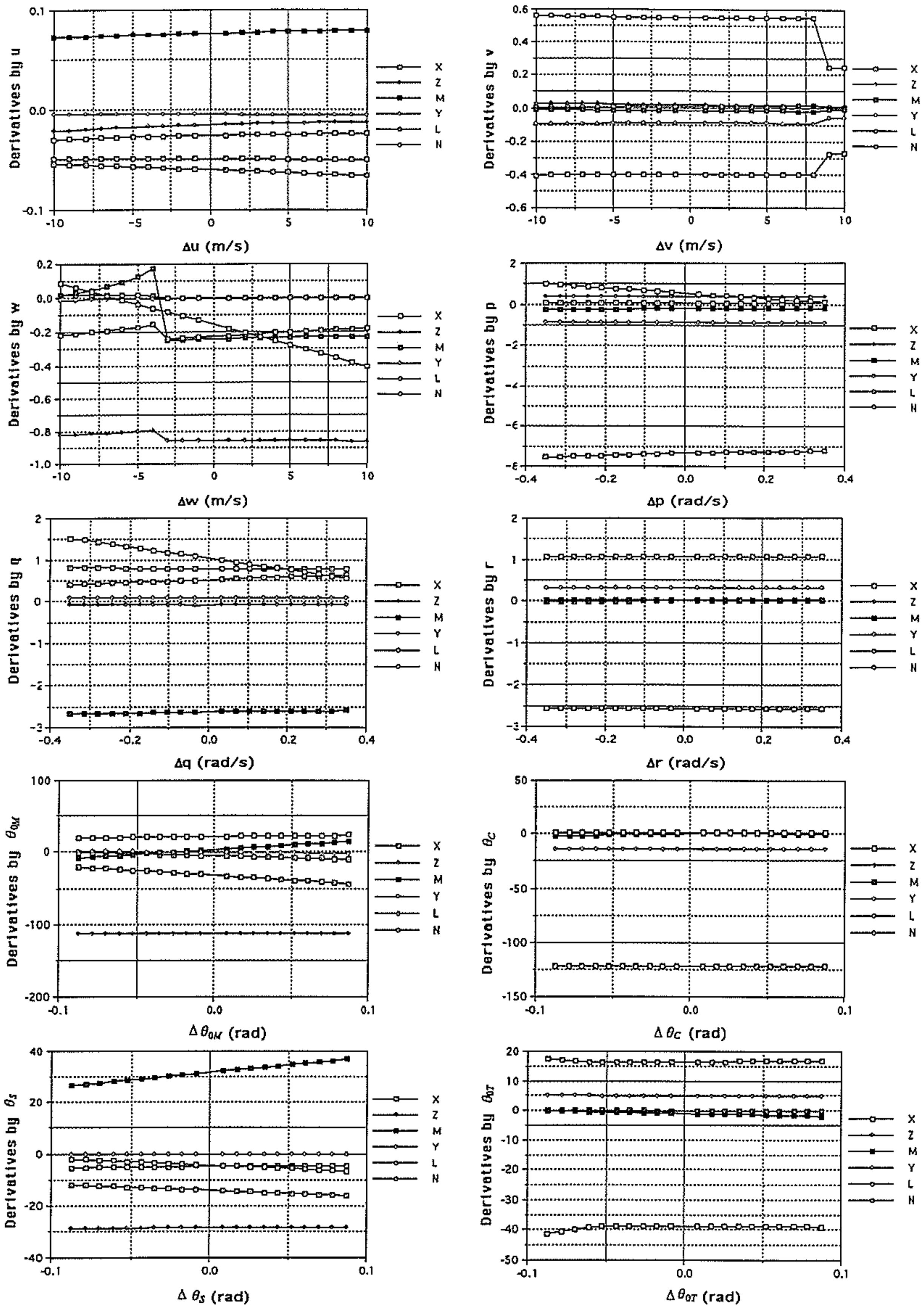

Figure 4 Numerically estimated derivatives at 70 kts level flight for Robinson R22

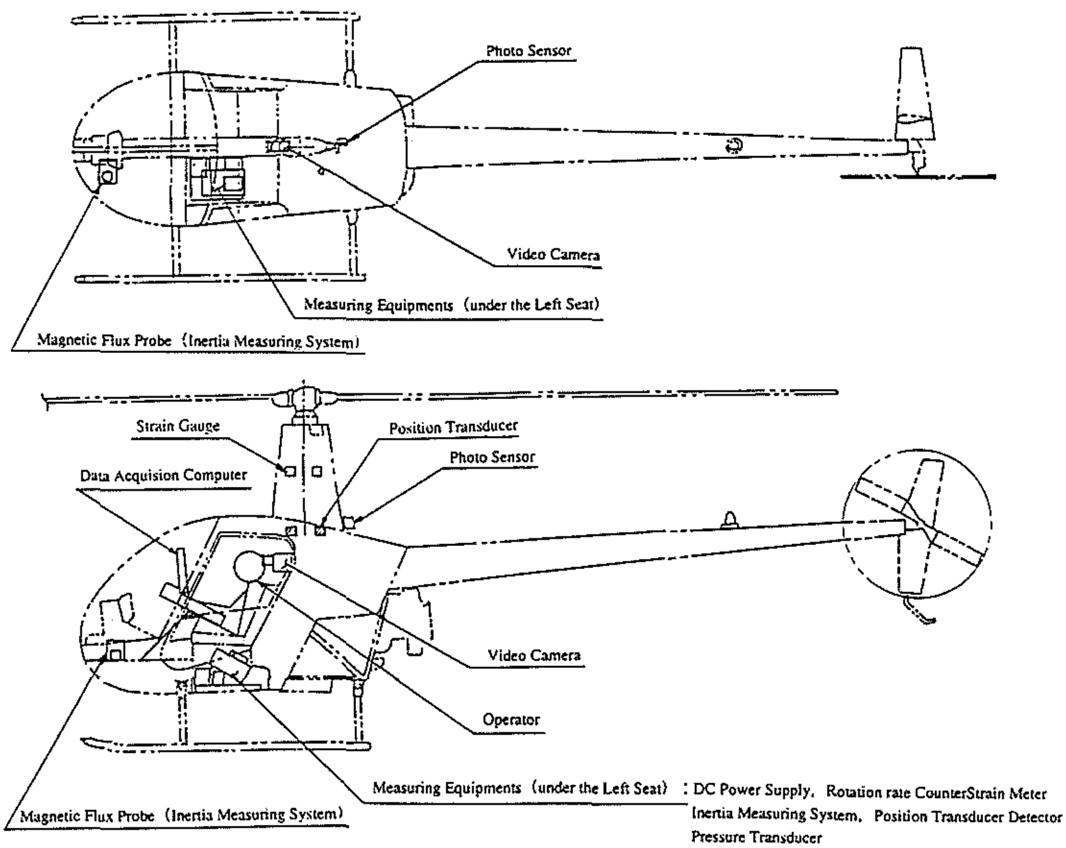

Figure 5 Layout of the data acquisition system on Robinson R22

copter near hovering flight. The highly nonlinear terms may have to be eliminated from the identification to improve the whole accuracy of other parameters. It seems that most nonlinear charateristics of the helicopter can be taken into account if squared state variables are included in the linearized equations.

3. Flight tests

Flight tests are carried out for Robinson R22 and Eurocopter AS 332 L-1 for the system identification and validation of the numerical results. The data acquisition system and measurement results are described in this section.

Data acquisition system

The whole data acquisition system was originally designed for installation in the limited space on the small two-seat helicopter Robinson R22. The weight left for the measuring system besides the test pilot and the operator is also restricted. As shown in Figure 5, the inertia measuring system, control input transducers, rotational speed of main rotor measuring device, control linkage rod stress transducers and data sampling and storing laptop computer system are included.

The inertia measuring system utilizes three rate gyros and three servo-accelometers with a magnetic flux detecting probe. The internal computer calculates and outputs the aircraft direction, roll and pitch angles, three axes angular velocities and three directional accelerations in real time. The sensor unit is installed in the luggage room under the operator's seat and the magnetic flux probe is placed in the fore floor of the cabin.

The pilot control inputs are measured with four position transducers linked to the control linkage rods. The extension of the cable rotates the spring loaded shaft which is coupled to the potentiometer to give a continuous voltage output proportional to the cable extension. Three position transducers are placed under the swashplate linked to the three main rotor pitch rods and another is linked to the

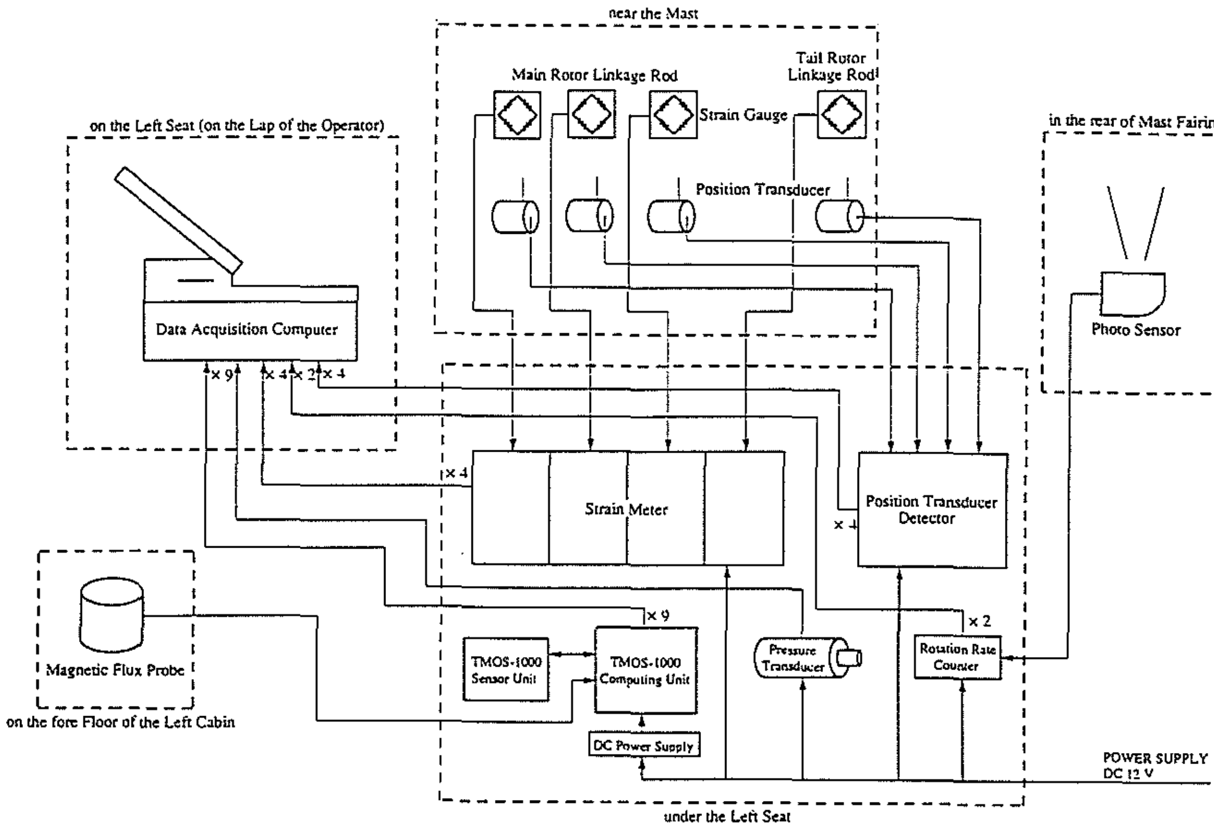

Figure 6 Wiring chart of the data acquisition sysitem

tail rotor pitch linkage rod. The relations between the outputs of transducers and the pitch angles of the blades are assumed linear and the coefficients are calibrated before the flight.

The rotational speed of main rotor is measured by a photo sensor located on the top of the fuselage beneath the main rotor blades. A random-reflective tape is placed on the lower surface of a blade. The passing blade turns the switch on/off to produce a pulse that is inputted to a counter to give a signal proportional to the rotational speed. The pulse itself indicates the blade azimuth position.

Data sampling and recording are performed with a laptop computer as the host and a 32-channel 12-bits resolution A/D converter connected to its extending buslines. The computer with its extending box was placed on the lap of the operator during the flight. Sampled data are initially stored into the computer's main memory and then written to the internal hard drive. The maximum sampling rate is 25μs, which is sufficient for the measurement of the helicopter motion.

The wiring chart of the data acquisition system is shown in Figure 6. This whole system can be driven independently with its own battery. The total weight of the whole data acquition system including the transducers and signal conditioners is less than 20 kg.

The same system was used for the flight test of AS 332 L-1. There was more vertical vibrations in the Super Puma cabin, especially in decent flight. However, the whole system worked very well without any trouble.

<u>Flight tests and measurement results</u>

Flight tests of Robinson R22 were carried out mainly for hovering and level flight. Only detailed hovering flight was performed for AS

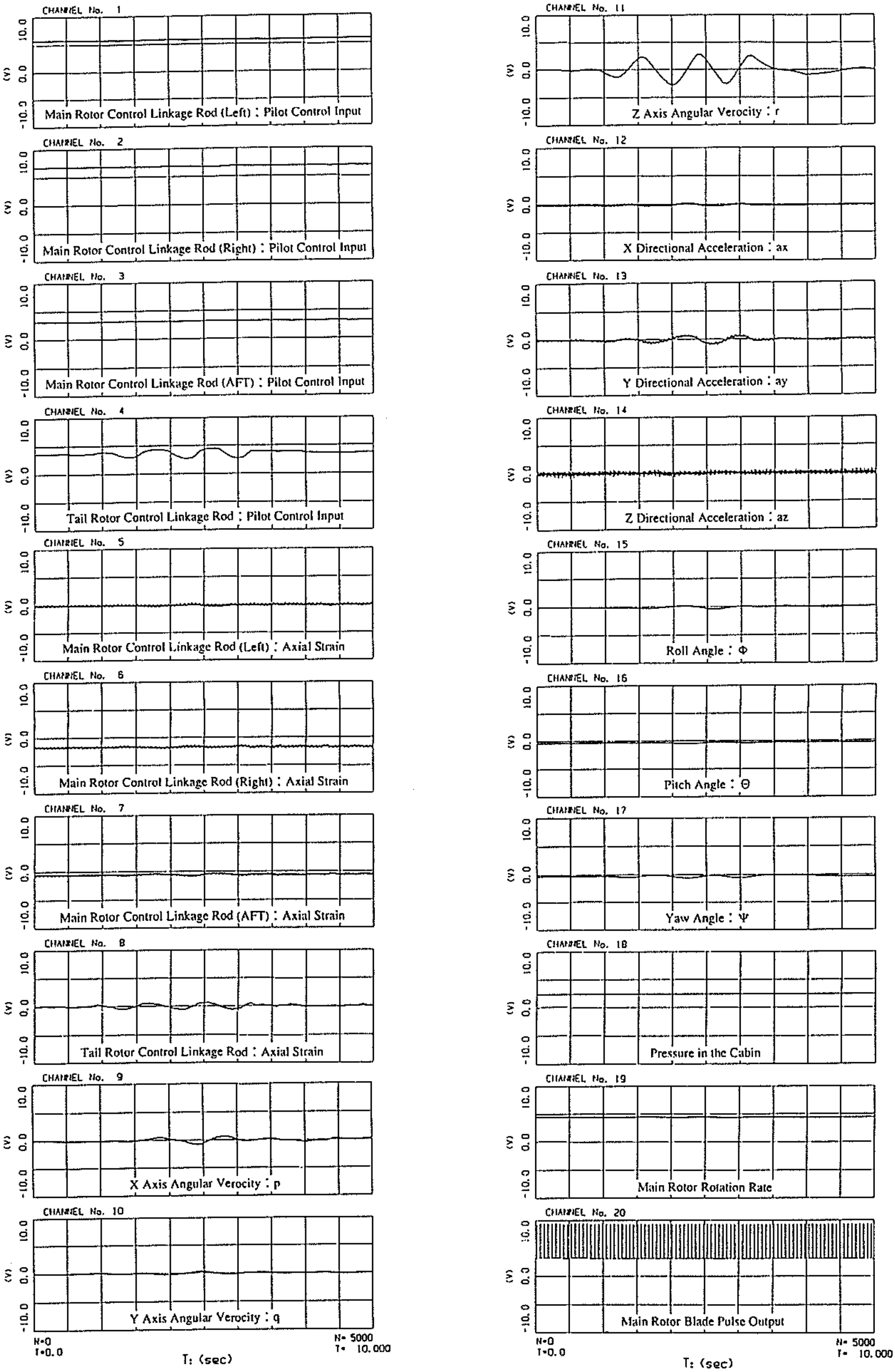

Figure 7 Sample of the measured data set for Robinson R22 near hovering flight

332 L-1. At each test maneuver, the pilot was asked to give either a sudden step or a periodic control input from trimmed flight. Four axes inputs, i.e. the collective up/down, longitudinal cyclic stick foward/back, lateral cyclic stick left/right sideway flight and the pedal directional control, were given separately. During a test maneuver, only one control was moved mainly, other controls were used in minimum to keep the helicopter in balance.

A sample of measured data set when the pilot was giving the helicopter periodic directional change is shown in Figure 7. Periodic roll motion can also be observed as one of the cross coupling effects.

Physical data were calculated from the measured voltages with corrections for the rate gyros and accelometers biases. The state variables *u, v* and *w* selected for the system identifications were integrated from the accelometers and rate gyros outputs. The duration for one disturbance control input is about 10 seconds. The inertia sensors used had good accuracy considering the large motions of the helicopter. The position deviation of the sensor unit from the center of gravity of the helicopter was compensated in the velocity integration.

4. System identification

From Eq.(3), write the known terms in left-hand side, we have

$$\dot{\mathbf{u}}(t) - \mathbf{C}_g\Theta(t) - \mathbf{C}_{u_0}\mathbf{p}(t) = \dot{\mathbf{u}}_0 + \mathbf{A}\mathbf{u}(t) + \mathbf{B}\theta(t) \quad (5)$$

Here the term $\dot{\mathbf{u}}_0$ is retained as the initial acceleration deviations from the ideal trim condition, which are unknowns and must be determined for each flight data. With this expression, it is difficult to identify all the coefficients in matrices **A** and **B** because there are mainly only one-axis disturbance in one data set.

System identification with frequency-response method has been performed for BO 105 and other helicopters[5,6]. If Eq.(5) is transformed into frequency domain, then we have

$$\omega\mathbf{u}(\omega) - \mathbf{C}_g\Theta(\omega) - \mathbf{C}_{u_0}\mathbf{p}(\omega) = \mathbf{A}\mathbf{u}(\omega) + \mathbf{B}\theta(\omega) \quad (6)$$

The deviations term $\dot{\mathbf{u}}_0$ diminished in this expression because they are constants. We can combine the different transformed datasets into one database to determine the most likely correct matrices **A** and **B**. Considering the pilot control input has only a limited frequency band, only the transformed data at low-end of the frequency axis are used in current system identification. Least square method was used to determine the coefficients in **A** and **B**.

Identification was also carried out when squared terms of state variables has been added to the linearized system. In such case, the resulted system is no longer linear. With these squared state variables included, the computed outputs meet with the flight test results better. However, there were no significant difference for the first order derivatives.

Identified results differs a lot depending on whether step responses or periodic responses are used. Considering the nature of small disturbance linearization, periodic responses are mainly used for current system identification, which also have more meaningful data on frequency domain.

5. Comparisons and discussions

For comparisons, main stability derivatives and control derivatives of R22 and AS 332 L-1 in hover are listed in Table 3.

The main control derivatives agree with each other quite well except for Y_{θ_C}. The rea-

Table 3 Comparisons of the analytical and identified derivatives in hover

	Robinson R22		AS 332 L-1	
Derivative	Analytical	Identification	Analytical	Identification
X_u	-0.032	-0.045	-0.045	-0.036
X_q	0.850	0.190	1.350	0.011
Z_w	-0.150	-0.052	-0.100	-0.130
Z_q	0.010	-0.250	0.005	0.570
M_u	0.050	-0.075	0.010	0.028
M_q	-2.100	-0.210	-0.480	-0.110
L_q	0.800	0.065	1.880	-0.102
Y_v	-0.030	-0.081	-0.050	-0.160
Y_p	-0.850	-0.089	1.000	0.610
L_v	-0.230	0.006	-0.065	-0.086
L_p	-7.500	-0.770	2.500	-1.030
N_v	0.100	0.210	0.020	0.057
N_r	-0.400	-0.060	-0.150	-0.690
M_p	-0.200	-0.200	0.250	0.150
$X_{\theta_{0M}}$	-2.400	-8.500	2.000	1.660
X_{θ_S}	-15.200	-7.200	-21.700	-8.570
$Z_{\theta_{0M}}$	-90.500	-92.100	-80.200	-59.100
M_{θ_S}	36.800	17.300	6.830	4.460
$Y_{\theta_{0M}}$	0.800	-2.500	1.800	4.950
Y_{θ_C}	-15.400	-0.740	22.100	0.880
$Y_{\theta_{0T}}$	4.400	4.680	-4.640	-5.130
L_{θ_C}	-136.300	-55.000	36.800	20.200
$N_{\theta_{0M}}$	33.400	8.800	-8.700	-9.040
$N_{\theta_{0T}}$	-34.200	-23.700	6.670	4.650

Table 4 Nondimensionalized derivatives in hover

	Robinson R22		AS 332 L-1	
Derivative	Analytical	Identification	Analytical	Identification
$\overline{X}_{\overline{u}}$	-0.05152	-0.07245	-0.06345	-0.05076
$\overline{X}_{\overline{q}}$	0.004165	0.000931	0.00621	0.0000506
$\overline{Z}_{\overline{w}}$	-0.2415	-0.08372	-0.141	-0.1833
$\overline{Z}_{\overline{q}}$	0.000049	-0.001225	0.000023	0.002622
$\overline{M}_{\overline{u}}$	26.42	-39.63	4.302	12.0456
$\overline{M}_{\overline{q}}$	-3.381	-0.3381	-0.6768	-0.1551
$\overline{L}_{\overline{q}}$	1.288	0.10465	2.6508	-0.14382
$\overline{Y}_{\overline{v}}$	-0.0483	-0.13041	-0.0705	-0.2256
$\overline{Y}_{\overline{p}}$	-0.004165	-0.0004361	0.0046	0.002806
$\overline{L}_{\overline{v}}$	-121.532	2.95904	-27.963	-36.9972
$\overline{L}_{\overline{p}}$	-12.075	-1.2397	3.525	-1.4523
$\overline{N}_{\overline{v}}$	52.84	110.964	8.604	24.5214
$\overline{N}_{\overline{r}}$	-0.644	-0.0966	-0.2115	-0.9729
$\overline{M}_{\overline{p}}$	-0.322	-0.322	0.3525	0.2115
$\overline{X}_{\overline{\theta}_{0M}}$	-0.01896	-0.06715	0.0158	0.013114
$\overline{X}_{\overline{\theta}_S}$	-0.12008	-0.05688	-0.17143	-0.067703
$\overline{Z}_{\overline{\theta}_{0M}}$	-0.71495	-0.72759	-0.63358	-0.46689
$\overline{M}_{\theta_S}$	95.312	44.807	13.5917	8.8754
$\overline{Y}_{\overline{\theta}_{0M}}$	0.00632	-0.01975	0.01422	0.039105
$\overline{Y}_{\overline{\theta}_C}$	-0.12166	-0.005846	0.17459	0.006952
$\overline{Y}_{\overline{\theta}_{0T}}$	0.03476	0.036972	-0.036656	-0.040527
$\overline{L}_{\overline{\theta}_C}$	-353.017	-142.45	73.232	40.198
$\overline{N}_{\overline{\theta}_{0M}}$	86.506	22.792	-17.313	-17.9896
$\overline{N}_{\overline{\theta}_{0T}}$	-88.578	-61.383	13.2733	9.2535

son for this discrepancy is not clear at this point.

Some of the numerically estimated stability derivatives are nonlinear in hover as discussed before. Only the nearly linear and dominant terms are listed in Table 3.

The nondimensionalized derivatives are listed in Table 4. It can be seen the state and control derivatives have the same order of magnitude for the same equation. However, the derivatives for the translational motion have completely different order of magnitude from that for the angular motions. This is the unique feature of rotary wing aircraft compared with the fixed wings[1].

Flight tests were carried out with care and the flight data are reliable. The disagreement between the analytical and system identified results need to be studied further. The linearized dynamics model obtained from both approaches have their own uncertainties. The stability analysis relys mainly on the state derivatives which showed large discrepancies between the analytical and flight test results. There exists a question on which result is more reliable. Theoretically, accuate state derivatives can be obtained with the desired state variable significantly disturbed while keeping other states and controls fixed. It is impossible to accomplish this condition in real flight, but this can easily be done with the computer simulation programs. Diftler[7] has used the linearized model obtained from the a flight simulation program to study the UH-80A stability augmentation system. However, as mentioned before, the linearization of the equations of motion itself limits its applicability. Careful check must be made to assure the computer program correctly simulates the real aircraft flight dynamics. The flight test data will play an important role for this task. After this check, direct nonlinear simulation of the flight dynamics of helicopter may become more important in the understanding of the helicopter flight characteristics and in the design of advanced automatic stabilization and control systems.

6. Concluding remarks

A set of nondimensional parameters for linearized helicopter flight dynamics has been proposed.

The derivatives are numerically estimated with perturbation method from a helicopter flight simulation program. It is shown that for a helicopter in hovering flight, some derivatives are highly nonlinear which may cause the linearized analysis lose effectiveness.

Flight tests were carried out for Robinson R22 and Eurocopter AS 332 L-1 helicopters. Comparisons of the analytical and identified derivatives are performed. It is shown that the control derivatives generally agree well. The stability derivatives had large discrepancies.

It is considered that accurate identification for the full set of stability derivatives are difficult because the nonlinear nature of the helicopter motion. Direct nonlinear analysis for the helicopter dynamics especially in hovering flight looks more promising.

Acknowledgments

The flight test of Robinson R22 Beta was performed by authors and the aircraft is owned by Kawada Industries, Inc. The flight test of AS 332 L-1 (Super Puma) was conducted by Tokyo Fire Department, Japan. The authors gratefully acknowledge their permission to use the flight test data for the present analysis.

References

1) Jay W. Fletcher, Identification of UH-60 Stability Derivative Models in Hover from

Flight Test Data, Proceeding of the American Helicopter Society 49th Annual Forum, May 1993, pp.183-210.
2) R.W.Prouty, Helicopter Performance, Stability, and Control, PWS Publishers, 1986.
3) H. Glauert, The Analysis of Experimental Results in the Windmill Brake and Vortex Ring States of an Airscrew, R&M 1026.
4) A. Azuma and A. Obata, Induced Flow Variation of the Helicopter Rotor Operating in the Vortex Ring State, J. Aircraft, Vol. 5, No. 4, pp. 381-386, 1968.
5) M.B. Tischler and M.G. Cauffman, Frequency-Response Method for Rotorcraft System Identification with Applications to the BO-105 Helicopter, paper presented at the 46th Annual Forum of the AHS, 1990.
6) M.J.A. Ham, Frequency Domain Flight Testing and Analysis of an OH-58D Helicopter, J. AHS, pp. 16-24, October 1992.
7) M.A. Diftler, UH-60A Helicopter Stability Augmentation Study, paper No.74 presented at 14th European Rotorcraft Forum, 1988.